

Synthesis and SAR of arylaminoethyl amides as noncovalent inhibitors of cathepsin S: P3 cyclic ethers

David C. Tully,* Hong Liu, Arnab K. Chatterjee, Phil B. Alper, Robert Epple, Jennifer A. Williams, Michael J. Roberts, David H. Woodmansee, Brian T. Masick, Christine Tumanut, Jun Li, Glen Spraggon, Michael Hornsby, Jonathan Chang, Tove Tuntland, Thomas Hollenbeck, Perry Gordon, Jennifer L. Harris and Donald S. Karanewsky

Genomics Institute of the Novartis Research Foundation, 10675 John J. Hopkins Dr., San Diego, CA 92121, USA

Received 18 May 2006; revised 7 July 2006; accepted 11 July 2006

Available online 28 July 2006

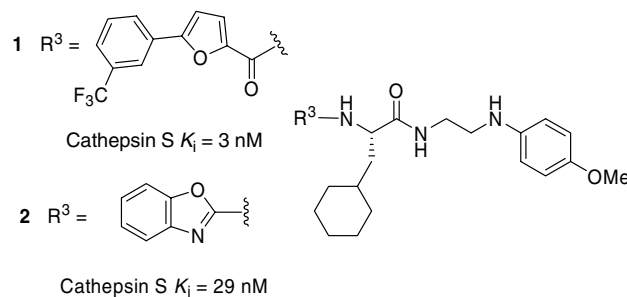
Abstract—The synthesis and structure–activity relationship of a series of arylaminoethyl amide cathepsin S inhibitors are reported. Optimization of P3 and P2 groups to improve overall physicochemical properties resulted in significant improvements in oral bioavailability over early lead compounds. An X-ray structure of compound **37** bound to the active site of cathepsin S is also reported.

© 2006 Elsevier Ltd. All rights reserved.

Cathepsin S (Cat S) is a cysteine protease expressed in antigen presenting cells such as B cells, dendritic cells, and macrophages. Cat S mediates proteolysis of the invariant chain that is associated with the major histocompatibility class II (MHC-II) complex.^{1–4} This proteolytic event is a prerequisite to productive loading of antigen onto the MHC-II complex, rendering cathepsin S an attractive therapeutic target for immunosuppression. The development of selective Cat S inhibitors for the modulation and regulation of immune hyperresponsiveness may provide a novel treatment for chronic conditions such as asthma, allergies, myasthenia gravis, and rheumatoid arthritis.^{5–7}

We have recently detailed the synthesis and SAR of arylaminoethyl amides that act as reversible, noncovalent inhibitors of Cat S.^{8–10} Compounds **1** and **2**, while potent and highly selective over related cathepsins K, L, B, F, and V, exhibit poor PK properties in rats. The lack of oral bioavailability of **1** and **2** is due in part to low solubility but also to high clearance stemming from poor metabolic stability of the compounds. Early

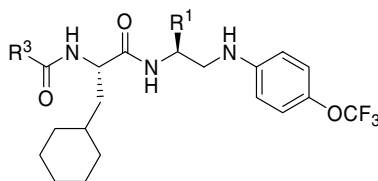
lead optimization of this series focused on improving the physicochemical and PK parameters, while preserving the potency and selectivity over related members of the cathepsin family.¹⁰ In this account, we describe the continued optimization of the P3 aryl amide subunit and the subsequent required modifications in P1 and P2.



Compounds **14–20** (Table 1), lacking a P1 alkyl substituent, were synthesized using the solid-phase procedure previously described.⁸ The 5-phenyl-2-furanoic amide motif in P3 generally confers excellent selectivity over cathepsins K and L (Table 1). The distal region of the S3 subsite of Cat S is defined by a flexible Lys64 residue which can re-orient its sidechain to accommodate the P3 moiety of the inhibitor.^{8,10,11} In contrast, the analogous region of the Cat L S3 pocket is

Keywords: Cathepsin S; Cysteine protease inhibitor; Noncovalent inhibitor; Peptidomimetic; X-ray structure.

* Corresponding author. Tel.: +1 8588121559; fax: +1 8588121648; e-mail: dtully@gnf.org

Table 1. Inhibition of cathepsins S, K, and L—optimization of P3^a

Compound	R ³	R ¹	K _i (μM)		
			Cat S	Cat K	Cat L
14	5-(3-CF ₃ phenyl)-2-furan	-H	0.011	8.58	4.97
15	5-(3-fluorophenyl)-2-furan	-H	0.034	11.7	4.08
16	2-Benzofuran	-H	0.017	0.150	0.045
17	2-Furan	-H	0.047	8.81	1.15
18	3-Furan	-H	0.006	9.34	0.914
19	(<i>R</i>)-2-Tetrahydrofuran	-H	0.658	>30	3.12
20	3-Tetrahydrofuran	-H	0.213	>30	7.94
21	(<i>R</i>)-2-Tetrahydrofuran	-Me	0.018	4.61	0.582
22	(<i>S</i>)-2-Tetrahydrofuran	-Me	0.053	>30	0.331
23	3-Tetrahydrofuran	-Me	0.021	>30	4.79
24	(<i>S</i>)-Tetrahydrofuran-3-yl-oxy	-Me	0.049	>30	0.594
25	(<i>R</i>)-Tetrahydrofuran-3-yl-oxy	-Me	0.042	>30	2.57
26	4-Tetrahydropyran	-Me	0.012	14.3	0.232
27	Tetrahydropyran-4-yl-oxy	-Me	0.012	13.3	0.075
28	1-Morpholine	-Me	0.011	1.66	0.125

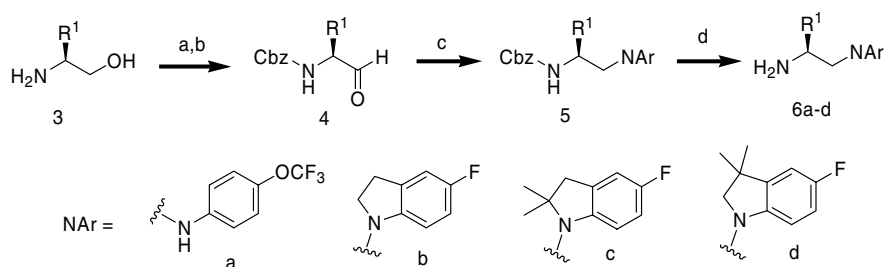
^a Details of the assay conditions can be found in the [Supplementary data](#). K_i values are means of at least three experiments.

occupied by a comparatively less flexible Glu63, which presumably sterically clashes with the distal phenyl ring of the P3 moiety in compounds **1**, **14**, and **15**.^{8,12} Substitutions on the distal phenyl ring such as small alkyl groups (**14**) and halogens (**15**) are generally well tolerated, usually preserving both the potency and selectivity. While the biaryl amide in the P3 position confers selectivity of the compounds over Cat L, this moiety also contributes to suboptimal physicochemical properties such as low aqueous solubility, high log*P*, and high molecular weight.

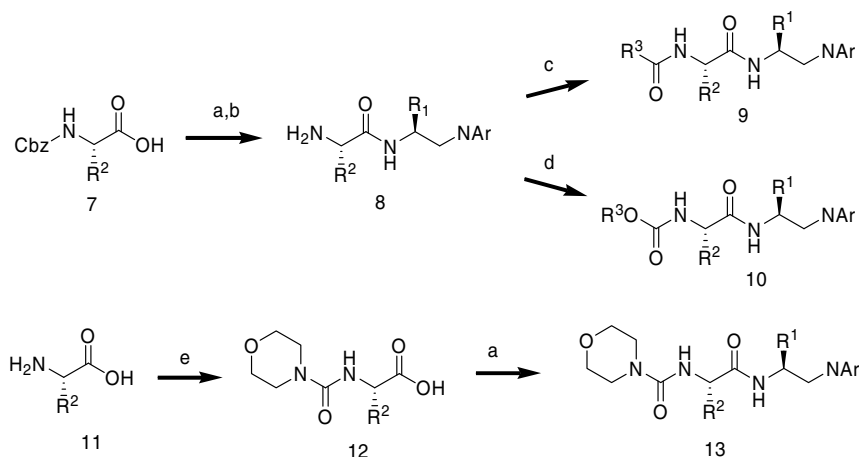
The syntheses of analogs bearing a P1 alkyl substituent are detailed in [Schemes 1 and 2](#). Commercially available (*S*)-2-amino-1-propanol **3** (or the corresponding butanol for R¹ = Me) was protected as the benzyl carbamate and then oxidized to the aldehyde **4** with Dess–Martin periodinane. Reductive amination with the appropriate aniline or indoline afforded **5**, which was then subjected to hydrogenolysis to provide the diamines **6a–d**.

Commercially available N-Cbz amino acids **7** were coupled to diamines **6a–d** with HATU-activation and deprotected under catalytic hydrogenation to provide **8**. Conversion to P3 **9** was achieved by HATU-mediated condensation of **8** with the appropriate carboxylic acid, while P3 carbamates **10** were prepared by acylation of **8** with the corresponding nitrophenylcarbonate. Morpholine ureas, **13**, were synthesized by acylation of the commercially available amino acids with morpholinecarbonyl chloride under Schotten–Bauman conditions, followed by peptide coupling with diamines **6a–d** ([Scheme 2](#)).

Results from our efforts to optimize the P3 fragment of this series are shown in [Table 1](#). Replacement of the biaryl amide with a fused bicyclic ring, such as benzofuran **16**, results in a significant loss of selectivity over cathepsins K and L. A similar trend with this series has also been observed with other fused heterocyclic P3 amides such as 2-naphthyl.⁸ When the distal aryl ring was



Scheme 1. Reagents: (a) benzyl chloroformate, Et₃N, CH₂Cl₂, 86%; (b) Dess–Martin periodinane, CH₂Cl₂; (c) HNAr (aniline or indoline), NaB(CN)H₃, AcOH, MeOH, 60–75% over two steps; (d) H₂, Pd/C, EtOH, 90–95%.



Scheme 2. Reagents: (a) **6a–d**, HATU, DIEA, CH₂Cl₂, 75–87%; (b) H₂, Pd/C, EtOH, 87–93%; (c) R³COOH, HATU, DIEA, CH₂Cl₂, 71–84%; (d) *para*-NO₂PhOCO₂R₃, DIEA, DMF, 44–63%; (e) morpholinecarbonylchloride, NaOH, H₂O, 42–67%.

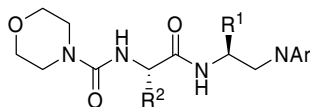
removed completely as in the 2-furyl analog, **17**, a potent cathepsin S inhibitor was obtained with modest selectivity (25×) over cathepsin L. The 3-furyl analog, **18**, not only improved the potency toward Cat S ($K_i = 6$ nM) but also the selectivity over Cat L (150×). We surmised that in the absence of a distal phenyl ring, the furan oxygen may engage the positively charged Lys64 sidechain to form a favorable electrostatic interaction. On the other hand, its affinity to Cat L may be penalized by the repulsive interaction with Glu63.

Saturation of the P3 furan ring to tetrahydrofurans **19** and **20** resulted in a considerable drop-off (>10×) in activity, presumably due to the loss of the π - π interaction between the furan ring and Phe70. Since the introduction of a cyclic ether was considered to have a greater potential for further improvement in solubility, we sought to optimize further upon this motif. We have previously shown that the introduction of an (*S*)-alkyl substituent onto the diamine section of this series as a P1 sidechain typically leads to an increase in potency.^{9,10} This was again observed to be the case, as the introduction of a methyl group (**19** → **21**) improved the activity by over 30-fold ($K_i = 18$ nM), while affording modest selectivity over cathepsin L. In comparing the absolute configurations in P3, the (*R*)-2-tetrahydrofuran diastereomer **21** was determined to be preferred over the (*S*)-diastereomer (**22**) by a factor of three. Tetrahydrofuran **23** was equipotent with **21** and gave a significant improvement in selectivity over both cathepsins K and L. With the improvements in solubility and metabolic stability over P3 aryl amides such as **1**, the PK parameters of tetrahydrofuran amides **21** and **23** were profiled in male Wistar rats (Table 3). Both compounds gave significant improvements in oral exposures over **1** and related compounds, and had oral bioavailabilities of 36% and 19%, respectively. When dosed intravenously, both compounds exhibited moderate clearance rates and terminal half-lives.

Continued investigation led to carbamates **24** and **25**, which were equipotent with respect to cathepsin S, with the *R*-isomer exhibiting a better selectivity profile

(Table 1). The increased ring size of tetrahydropyran **26** resulted in a more potent cathepsin S inhibitor ($K_i = 12$ nM) with modest (~20×) selectivity over cathepsin L. The tetrahydropyran analog, **27**, and the morpholine analog, **28**, each provided equally potent cathepsin S inhibitors with solid selectivity over Cat K, but narrowing windows of selectivity over Cat L.

Six-membered rings such as pyran or morpholine in the P3 position of this series appeared to be the most beneficial for improving the *in vitro* potency. We therefore opted to fix this position as the morpholine urea, represented by **28**, and investigated the SAR of the P2 substituent in an effort to improve selectivity. Several analogs with different P2 and P1 substituents are listed in Table 2. When the P1 alkyl group was increased to ethyl (**29**) or 2-methanesulfonyl-ethyl (**30**), a considerable boost in inhibitory activity toward both Cat K and Cat L resulted, significantly reducing the selectivity. Alternatively, when the P1 alkyl group was removed entirely (**31**) the activity dropped off proportionally across each enzyme tested. Interestingly, while cathepsin S generally tolerates both aliphatic and aromatic hydrophobic groups in the S2 binding pocket, the benzyl analog, **32**, was not particularly active ($K_i = 11.4$ μ M) when combined with morpholine in P3. This is in contrast to previous SAR from this series in which substituted phenylalanines in P2 in combination with a benzamide P3 gave potent Cat S inhibitors.⁸ The *tert*-butyl alanine P2 was tolerated by Cat S (**33** and **34**); however, the selectivity over Cat K was only marginal. Cyclopentyl alanine **35** was four times less potent than cyclohexyl alanine **28**; however, its selectivity over Cat L was significantly improved (>50×). Compound **36**, derived from benzylcysteine, was equipotent to **28** and had an improved selectivity profile. The potent sulfone analog **37** ($K_i = 32$ nM) was completely inactive against cathepsins K, L, B, F, H, V, and X in the concentration ranges tested (>30 μ M). Unfortunately, compared to amides **21** and **23**, urea **37** had only modest oral bioavailability ($F = 16\%$) despite improved *in vitro* metabolic stability and solubility at pH 6.8 (Table 3).

Table 2. Inhibition of cathepsins S, K, and L—optimization of P2^a

Compound	R ²	R ¹	NAr ^b	K _i (μM)		
				Cat S	Cat K	Cat L
28	Cyclohexylmethyl	–Me	a	0.011	1.66	0.125
29	Cyclohexylmethyl	–Et	a	0.011	0.130	0.006
30	Cyclohexylmethyl	–CH ₂ CH ₂ SO ₂ Me	a	0.005	0.139	0.004
31	Cyclohexylmethyl	–H	a	0.099	18.8	2.11
32	PhCH ₂ –	–H	a	11.4	>100	>100
33	<i>tert</i> -Butylmethyl	–H	a	0.220	1.33	>30
34	<i>tert</i> -Butylmethyl	–Me	a	0.093	0.461	14.6
35	Cyclopentylmethyl	–Me	a	0.049	1.54	2.59
36	PhCH ₂ SCH ₂ –	–Me	a	0.012	2.48	1.18
37	PhCH ₂ SO ₂ CH ₂ –	–Me	a	0.032	>100	>30
38	Cyclohexylmethyl	–Me	b	0.087	5.13	0.512
39	Cyclohexylmethyl	–Me	c	0.111	13.1	1.06
40	Cyclohexylmethyl	–Me	d	0.011	16.9	0.810

^a Details of the assay conditions can be found in the [Supplementary data](#). K_i values are means of at least three experiments.

^b Structures of *N*-aryl moieties a–d are shown in [Scheme 1](#).

Table 3. Pharmacokinetics of selected analogs^a

Compound	clog <i>P</i>	In vitro		Single iv dose (3 mg/kg)			Single po dose (10 mg/kg)			
		Sol. pH = 6.8 (mg/mL)	RLM (% remaining)	<i>t</i> _{1/2} (min)	Cl (mL/min/kg)	<i>V</i> _{ss} (L/kg)	AUC (min μg/mL)	<i>C</i> _{max} (nM)	<i>t</i> _{1/2} (min)	<i>F</i> (%)
1	7.2	<0.001	12	—	—	—	3	19	146	—
2	5.8	0.010	4	288	11	1.63	0.9	12	318	<1
21	5.3	0.025	66	66	35	1.78	105	1237	58	36
23	5.0	0.030	56	108	39	2.48	49	491	90	19
37	3.2	0.043	100	49	39	0.87	42	639	66	16
40	6.3	0.010	<1	43	52	1.76	8	118	51	4

^a Pharmacokinetic data in male Wistar rats, where values are means of three individual experiments.

We have previously shown that the aniline moiety can be replaced by 5-fluoroindoline and derivatives thereof without significant loss in activity in the context of analogs bearing benzamide⁹ or heteroaryl¹⁰ P3 units. In combination with the morpholine P3 group, however, replacement of the aniline with 5-fluoroindoline (**38**) or 5-fluoro-2,2-dimethylindoline (**39**) resulted in nearly an order of magnitude loss in activity. The 5-fluoro-3,3-dimethylindoline (**40**) did however retain potency toward Cat S, as well as improve the selectivity over Cat L. Despite the favorable shift in the biochemical selectivity profile, substitution of the aniline P1' moiety had a deleterious effect on the PK parameters as demonstrated by **40**, which had low oral bioavailability and high clearance, likely due to enhanced first-pass metabolism, as suggested by poor *in vitro* metabolic stability.

We previously reported an X-ray structure of cathepsin S produced by soaking compound **2** with crystals of Cat S.¹⁰ This structure clearly showed the P1, P2, and P3 subsites of compound **2** bound to the active site of Cat S, but the P1' aniline group was disordered. An X-ray structure of Cat S with compound **37** was produced by soaking in the same manner, but yet again we were

unable to resolve electron density for the P1' aniline moiety.¹³ To further investigate this phenomenon and to determine whether the prime-side aniline moiety could be resolved, we endeavored to grow co-crystals of Cat S in the presence of **37**. Out of a broad screen consisting of 480 different buffer conditions, co-crystals of cathepsin S and **37** grew in a well containing 0.2M Zn(OAc)₂.¹³ The X-ray co-crystal structure was solved, and the crystals diffracted to 1.8 Å resolution and belonged to space group R3. This co-crystal structure clearly shows **37** bound to the active site of the enzyme ([Fig. 1](#)). Clear electron density for all atoms in the inhibitor was evident for both molecules in the asymmetric unit. It is apparent from this structure that Zn²⁺ has co-crystallized with the inhibitor and protein. The bound Zn²⁺ is tetrahedrally coordinated via the thiol group of the catalytic cysteine (Cys25), the imidazole sidechain of His164, the aniline nitrogen of **37**, and a chloride ion. It is unclear whether this interaction between the Cys25 thiolate, zinc dication, and the aniline is necessary for the formation of a stable co-crystal complex, or whether it is merely an artifact of the co-crystallization conditions with the inhibitor in the presence of a high concentration of Zn²⁺. We have further verified

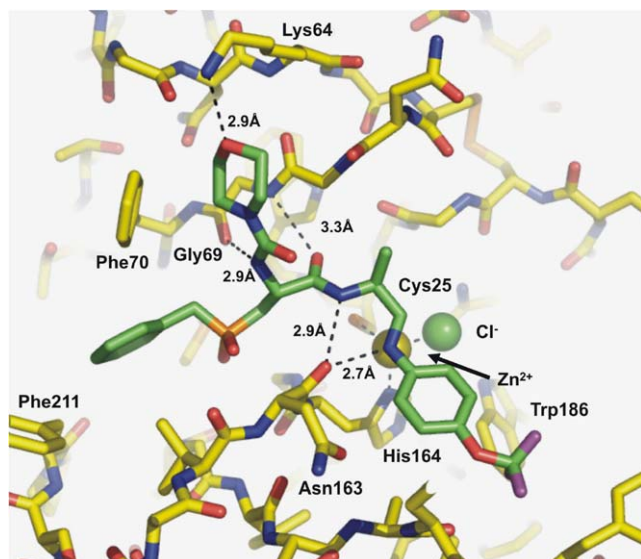


Figure 1. Crystal structure of cathepsin S at 1.8 Å co-crystallized with compound 37 (RCSB PDB ID: 2HH5). Protein carbon atoms are colored yellow whilst those of the inhibitor are green, oxygens are red, nitrogens blue, sulfurs orange, and fluorine violet. The Zn^{2+} ion is colored bronze whilst the chloride anion is colored green. Hydrogen bonds are indicated by dashed black and white lines. Figure generated using Pymol (<http://www.pymol.org>).

that Zn^{2+} is not required for in vitro inhibition of Cat S in our biochemical assays.¹⁴ This was accomplished by adding 2 μM $ZnCl_2$ to the assay buffer in the presence of and in the absence of 1 mM EDTA. In each case, the measured K_i s were unchanged relative to the standard assay buffer conditions.

There are a number of similarities between this structure and the previously reported X-ray structures of inhibitors bearing covalent warheads bound to cathepsin S,^{11,15,16} particularly in the S3 and S2 subsites. The P3 morpholine urea assumes a chair conformation and occupies the S3 pocket which is well defined by the backbone of Gly69 and the sidechains of Phe70 and Lys64. The sidechain ammonium group of Lys64 makes a favorable electrostatic interaction with the morpholine oxygen in each case. In the present structure, the ammonium nitrogen atom of Lys64 is 2.9 Å from the morpholine oxygen, which is close enough to establish a direct hydrogen-bond. However due to the inherent flexibility of this sidechain, this is more likely simply a favorable electrostatic interaction. The S2 pocket of Cat S is a deep hydrophobic cleft defined by the sidechains of Phe70, Met71, Val162, and Phe211. The large benzyl-sulfone P2 moiety is easily accommodated by the conformational switching of the flexible Phe211, which can adopt an open conformation to make room for inhibitors with larger P2 groups.¹¹ The aniline moiety clearly occupies the proximal S1' subsite lined by key residues Ala140, Arg141, and Asn163. The indole ring of Trp186 is situated at the base of the S1' pocket, and it stacks edge-on with the aniline group of the inhibitor. This P1' aniline moiety essentially occupies the analogous region of space as does the phenyl sulfone moiety of the irreversible inhibitor LHVS in the co-crystal structure reported by Pauly et al.¹¹

This report summarizes the SAR of a potent series of noncovalent cathepsin S inhibitors and highlights changes leading to improvements in oral bioavailability. The hydrophobic biaryl amide P3 substituent of **1**, an early lead compound, was replaced by aliphatic cyclic ethers, resulting in compounds with improved physicochemical properties and in vitro rodent microsomal stability. This led to major improvements in PK with analogs such as **21** being 36% orally bioavailable in rats.

Acknowledgments

The authors acknowledge Kirk Clark and Raviraj Kulathila (Novartis Institutes for Biomedical Research) for valuable discussions.

Supplementary data

Supplementary data associated with this article can be found, in the online version, at [doi:10.1016/j.bmcl.2006.07.033](https://doi.org/10.1016/j.bmcl.2006.07.033).

References and notes

- (a) Riese, R. J.; Mitchell, R. N.; Villadangos, J. A.; Shi, G. P.; Palmer, J. T.; Karp, E. R.; De Sanctis, G. T.; Ploegh, H. L.; Chapman, H. A. *J. Clin. Invest.* **1998**, *101*, 2351; (b) Villadangos, J. A.; Bryant, R. A. R.; Deussing, J.; Driessen, C.; Lennon-Duménil, A.-M.; Riese, R. J.; Roth, W.; Saftig, P.; Shi, G. P.; Chapman, H. A.; Peters, C.; Ploegh, H. L. *Immunol. Rev.* **1999**, *172*, 109; (c) Shi, G. P.; Villadangos, J. A.; Dranoff, F.; Small, C.; Gu, L.; Haley, K. J.; Riese, R.; Ploegh, H. L.; Chapman, H. A. *Immunity* **1999**, *10*, 197.
- (a) Nakagawa, T. Y.; Rudensky, A. Y. *Immunol. Rev.* **1999**, *172*, 121; (b) Honey, K.; Rudensky, A. Y. *Nat. Immunol.* **2003**, *3*, 472.
- Beers, C.; Burich, A.; Kleijmeer, M. J.; Griffith, J. M.; Wong, P.; Rudensky, A. Y. *J. Immunol.* **2005**, *174*, 1205.
- (a) Riese, R. J.; Wolf, P. R.; Brömme, D.; Natkin, L. R.; Villadangos, J. A.; Ploegh, H. L.; Chapman, H. A. *Immunity* **1996**, *4*, 357; (b) Driessen, C.; Bryant, R. A. R.; Lennon-Duménil, A.-M.; Villadangos, J. A.; Bryant, P. W.; Shi, G.-P.; Chapman, H. A.; Ploegh, H. L. *J. Cell Biol.* **1999**, *147*, 775.
- Yang, H.; Kala, M.; Scott, B. G.; Goluszko, E.; Chapman, H. A.; Christadoss, P. *J. Immunol.* **2005**, *174*, 1729.
- Nakagawa, T. Y.; Brissette, W. H.; Lira, P. D.; Griffiths, R. J.; Petrushova, N.; Stock, J.; McNeish, J. D.; Eastman, S. E.; Howard, E. D.; Clarke, S. R. M.; Rosloniec, E. F.; Elliott, E. A.; Rudensky, A. Y. *Immunity* **1999**, *10*, 207.
- (a) Thurmond, R. L.; Sun, S.; Karlsson, L.; Edwards, J. P. *Curr. Opin. Investig. Drugs* **2005**, *6*, 473; (b) Leroy, V.; Thurairatnam, S. *Expert Opin. Ther. Patents* **2004**, *14*, 301.
- Liu, H.; Tully, D. C.; Epple, R.; Bursulaya, B.; Li, J.; Harris, J. L.; Williams, J. A.; Russo, R.; Tumanut, C.; Roberts, M. J.; Alper, P. B.; He, Y.; Karanewsky, D. S. *Bioorg. Med. Chem. Lett.* **2005**, *15*, 4979.
- Alper, P. B.; Liu, H.; Chatterjee, A. K.; Nguyen, K. T.; Tully, D. C.; Tumanut, C.; Li, J.; Harris, J. L.; Tuntland, T.; Chang, J.; Gordon, P.; Hollenbeck, T.; Karanewsky, D. S. *Bioorg. Med. Chem. Lett.* **2006**, *16*, 1486.

10. Tully, D. C.; Liu, H.; Alper, P. B.; Chatterjee, A. K.; Epple, R.; Roberts, M. J.; Williams, J. A.; Nguyen, K. T.; Woodmansee, D. H.; Tumanut, C.; Li, J.; Spraggon, G.; Harris, J. L.; Chang, J.; Tuntland, T.; Karanewsky, D. S. *Bioorg. Med. Chem. Lett.* **2006**, *16*, 1975.
11. Pauly, T. A.; Sulea, T.; Ammirati, M.; Sivaraman, J.; Danley, D. E.; Griffor, M. C.; Kamath, A. V.; Wang, I. K.; Laird, E. R.; Seddon, A. P.; Menard, R.; Cygler, M.; Rath, V. L. *Biochemistry* **2003**, *42*, 3203.
12. Marquis, R. W.; James, I.; Zeng, J.; Trout, R. E. L.; Thompson, S.; Rahman, A.; Yamashita, D. S.; Xie, R.; Ru, Y.; Gress, C. J.; Blake, S.; Lark, M. A.; Hwang, S.-M.; Tomaszek, T.; Offen, P.; Head, M. S.; Cummings, M. D.; Veber, D. F. *J. Med. Chem.* **2005**, *48*, 6870.
13. [Supplementary data](#) contains details of co-crystallization conditions for the structure shown in [Figure 1](#) (RCSB PDB ID: 2HH5) as well as a second solved X-ray structure produced by soaking compound **37** with crystals of Cat S in the absence of Zn²⁺ (P1' subsite of inhibitor is disordered, RCSB PDB ID: 2HHN).
14. Experimental details of the biochemical assays are included as [Supplementary data](#).
15. Mcgrath, M. E.; Palmer, J. T.; Bromme, D.; Somoza, J. R. *Protein Sci.* **1998**, *7*, 1294.
16. Ward, Y. D.; Thomson, D. S.; Frye, L. L.; Cywin, C. L.; Morwick, T.; Emmanuel, M. J.; Zindell, R.; McNeil, D.; Bekkali, Y.; Giradot, M.; Hrapchak, M.; DeTuri, M.; Crane, K.; White, D.; Pav, S.; Wang, Y.; Hao, M.-H.; Grygon, C. A.; Labadia, M. E.; Freeman, D. M.; Davidson, W.; Hopkins, J. L.; Brown, M. L.; Spero, D. M. *J. Med. Chem.* **2002**, *45*, 5471.